Molecular Vision 2023; 29:274-288 <http://www.molvis.org/molvis/v29/274>
Received 22 January 2023 | Accepted 2 November 2023 | Published 6 November 2023

Changes in glutamate and glutamine distributions in the retinas of cystine/glutamate antiporter knockout mice

Luis J. Knight,[1,3] Renita M. Martis,[1,2,3] Paul J. Donaldson,[1,3] Monica L. Acosta,[2,3,4] Julie C. Lim[1,3,4]

[1]Department of Physiology, School of Medical Sciences, University of Auckland; [2]School of Optometry and Vision Science, University of Auckland; [3]New Zealand National Eye Centre, University of Auckland, New Zealand; [4]Centre for Brain Research, University of Auckland, New Zealand

Purpose: The cystine/glutamate antiporter is involved in the export of intracellular glutamate in exchange for extracellular cystine. Glutamate is the main neurotransmitter in the retina and plays a key metabolic role as a major anaplerotic substrate in the tricarboxylic acid cycle to generate adenosine triphosphate (ATP). In addition, glutamate is also involved in the outer plexiform glutamate-glutamine cycle, which links photoreceptors and supporting Müller cells and assists in maintaining photoreceptor neurotransmitter supply. In this study, we investigated the role of xCT, the light chain subunit responsible for antiporter function, in glutamate pathways in the mouse retina using an xCT knockout mouse. As xCT is a glutamate exporter, we hypothesized that loss of xCT function may influence the presynaptic metabolism of photoreceptors and postsynaptic levels of glutamate.

Methods: Retinas of C57BL/6J wild-type (WT) and xCT knockout (KO) mice of either sex were analyzed from 6 weeks to 12 months of age. Biochemical assays were used to determine the effect of loss of xCT on glycolysis and energy metabolism by measuring lactate dehydrogenase activity and ATP levels. Next, biochemical assays were used to measure whole-tissue glutamate and glutamine levels, while silver-intensified immunogold labeling was performed on 6-week and 9-month-old retinas to visualize and quantify the distribution of glutamate, glutamine, and related neurochemical substrates gamma-aminobutyric acid (GABA) and glycine in the different layers of the retina.

Results: Biochemical analysis revealed that loss of xCT function did not alter the lactate dehydrogenase activity, ATP levels, or glutamate and glutamine contents in whole retinas in any age group. However, at 6 weeks of age, the xCT KO retinas revealed altered glutamate distribution compared with the age-matched WT retinas, with accumulation of glutamate in the photoreceptors and outer plexiform layer. In addition, at 6 weeks and 9 months of age, the xCT KO retinas also showed altered glutamine distribution compared with the WT retinas, with glutamine labeling significantly decreased in Müller cell bodies. No significant difference in GABA or glycine distribution were found between the WT and xCT KO retinas at 6 weeks or 9 months of age.

Conclusion: Loss of xCT function results in glutamate metabolic disruption through the accumulation of glutamate in photoreceptors and a reduced uptake of glutamate by Müller cells, which in turn decreases glutamine production. These findings support the idea that xCT plays a role in the presynaptic metabolism of photoreceptors and postsynaptic levels of glutamate and derived neurotransmitters in the retina.

The retina has high and fluctuating energy demands that require adenosine triphosphate (ATP) generation through glycolysis and oxidative phosphorylation. Furthermore, a high rate of lactate production via aerobic glycolysis occurs in the retina. Lactate is further metabolized to pyruvate by the enzyme lactate dehydrogenase (LDH) to support ATP production via the tricarboxylic acid (TCA) cycle [1,2]. The high energy demand of the retina is supported by anaplerotic reactions, which replenish the TCA cycle intermediates at the expense of neurotransmitters. Glutamate, the most prevalent excitatory neurotransmitter in the retina [3,4], is a critical anaplerotic substrate that is converted to α-ketoglutarate by glutamate dehydrogenase to help drive ATP production and reduce reliance on aerobic glycolysis. Glutamate is synthesized from its precursor amino acid glutamine via the glutamate-glutamine cycle [5,6]. Glutamate released at the photoreceptor synapse is taken up by Müller cells (MCs) and converted to glutamine. In MCs, glutamine is exported and taken up by the photoreceptors and converted back to glutamate, allowing the photoreceptors to recycle and reuse glutamate for several purposes, including neurotransmission and ATP production via the TCA cycle, while in the inner retina, glutamate is also used for the synthesis of other neurotransmitters such as gamma aminobutyric acid (GABA).

Owing to the importance of glutamate in the retina, glutamate and its precursor, glutamine, are tightly restricted and compartmentalized in retinal cells. As glutamate is the primary excitatory neurotransmitter in the retina, glutamate

Correspondence to: Julie C Lim, Department of Physiology, School of Medical and Health Sciences, University of Auckland, 85 Park Road, Grafton 1023, Auckland, New Zealand; email: j.lim@auckland.ac.nz

immunoreactivity is observed in the photoreceptors, bipolar (BP) cells, and ganglion cells (GCs) that form the direct synaptic transmission pathway to the optic nerve [7]. However, glutamine is predominantly observed in MCs, as similar to astrocytes in central nervous tissues, they are the only cells to express glutamine synthase and are therefore the exclusive source of glutamine for glutamate synthesis for BP and GCs [8-12]. This "metabolic compartmentation" allows neurochemical levels to be tightly controlled and regulated through glutamate-glutamine cycling. Given the important roles of glutamate in the retina, we hypothesized that glutamate transporters may influence the metabolism of photoreceptors and postsynaptic cells exposed to changes in glutamate levels.

The light chain subunit of the cystine/glutamate antiporter ("system xc-"), xCT, is involved in the exchange of extracellular cystine for intracellular glutamate. In the brain, xCT mediates the uptake of cystine, where it is rapidly reduced to cysteine for the synthesis of the major cellular antioxidant glutathione (GSH), an important line of defense against oxidative stress. In addition, the obligatory export of intracellular glutamate via xCT has been demonstrated to be a pathway of non-vesicular, Ca^{2+}-independent release of glutamate for glutamate signaling in neuronal tissues [13,14]. In the brain, the degree to which glutamate is released from xCT is controversial. However, Warr et al. showed that in Purkinje cells, while the density of xCT was between 10% and 75% of that of Na^{+}-dependent transporters, glutamate released through xCT did not have a significant effect on postsynaptic Purkinje cell membrane currents under physiological conditions [15]. This finding was supported by Cavelier and Attwell [16], who demonstrated that under physiological cystine concentrations, xCT was not a major contributor of glutamate release in the hippocampus. However, by increasing extracellular cystine concentrations, xCT played a more significant role in glutamate release [16].

By contrast, other studies have shown that in the hippocampus, striatum, and substantia nigra in models of loss of xCT function, extracellular glutamate levels ranged from 60% to 70% lower than those of their WT counterparts [17-19]. xCT has been localized to the photoreceptor ribbon synapse in the outer plexiform layer in rat, cow, chicken, and monkey retinas [20]. In addition, in the rat retina, the addition of exogenous cystine to elicit xCT function resulted in glutamate export and the subsequent opening of post-synaptic BP cell glutamate receptors visualized through the accumulation of the cation channel probe agmatine. This suggests that xCT plays a significant role in retinal glutamatergic signaling [20]. To evaluate the role of xCT on the metabolism of photoreceptors and postsynaptic glutamate levels in the retina, in this study, we examined the impact of loss of xCT function on the glycolytic pathway, ATP production, and amino acid distribution in WT and xCT KO retinas.

METHODS

Animals: All animals were treated in accordance with protocols approved by the University of Auckland Animal Ethics Committee (ethics application No. R001413), and the Association for Research in Vision and Ophthalmology statement for the Use of Animals in Ophthalmic and Vision Research. The xCT KO mice used in this study were previously described by Martis et al. [21] and were descendants of the global xCT KO strain developed by Sato et al. (2005) [22]. All xCT KO mice exhibited normal, healthy appearances, were fertile, and had normal lifespans when compared with their WT counterparts [22]. WT C57BL/6J mice were used as control animals and obtained from the Vernon Jansen Unit at the University of Auckland. Animals of either sex were used and studied at 6 weeks (young), 3 months (young adult), 6 months (adult), 9 months (middle age), and 12 months (old) of age. For LDH, ATP, and glutamate/glutamine assays, 6 animals (2 retinas from each animal pooled together) were evaluated for each age group (6 weeks to 12 months; n = 6). For immunogold labeling, 6 retinas were used for each label in both 6-week and 9-month age groups. For immunogold labeling, 6-week and 9-month-old animals were selected given the increased prevalence of subretinal deposits in the xCT KO retinas compared with the WT retinas at 9 months of age (but not at 12 months of age) [21].

Genotyping: Genotyping was performed as described by Sato et al. [22] and verified using polymerase chain reaction (PCR) of DNA extracted from the tail, as previously described [23]. Lack of xCT mRNA or protein expression in xCT KO mice was confirmed using PCR and western blotting [23]. In addition, the absence of the rd8 mutation, which leads to the presence of retinal lesions, was verified using PCR analysis with specific primers for the WT and rd8 alleles, as previously described [24].

Retina collection and tissue preparation: The mice were euthanized with CO_2 asphyxiation followed by cervical dislocation to ensure death before enucleation of the eyes. The eyes were dissected in ice-cold phosphate-buffered saline to prevent metabolite degradation, and the posterior eyecups were separated from the cornea within 1 minute. For biochemical assays, the sclera, choroid, and retinal pigment epithelium (RPE) were removed, and retinas were placed in 0.9% saline solution (for LDH activity and ATP assays) or a 50 mM Tris and 0.6N HCl homogenization buffer (for

glutamate and glutamine assays). The retinas were then homogenized, and the protein concentration was determined using a Direct Detect Infrared Spectrometer (Merck Millipore, Darmstadt, Germany). For immunohistochemistry experiments, the eyecup was placed in 1% paraformaldehyde with 2.5% glutaraldehyde for 60 min and then embedded in eponate resin in accordance with established protocols [25].

Lactate dehydrogenase activity: Total retinal lactate dehydrogenase (LDH) activity was measured using a modified commercial LDH activity assay kit (cytotoxicity detection kit [LDH]; catalog no. 11,644,793,001, Roche, Penzberg, Germany). Each retina was homogenized in 0.9% saline solution and centrifuged at 5,000×*g* for 7 min at 4°C, and the supernatant was collected. LDH activity was calculated on the basis of the rate of conversion of NAD^+ to NADH and the production of formazan salt in the presence of diaphorase catalyst, iodotetrazolum chloride, and sodium lactate. Absorbance was measured at 490 nm four times for 15 min using an Enspire Multimode Plate Reader (PerkinElmer, Waltham, MA). Standards and sample absorbance were measured in triplicate, and activity is expressed as units/ml.

ATP concentration: Total retinal ATP concentration was measured using a commercial assay kit (Adenosine 5′-triphosphate [ATP] Bioluminescent assay kit, catalog no. FLAA, Sigma-Aldrich, Saint Louis, MO). Samples were homogenized in 0.9% saline solution and centrifuged at 5000×*g* for 7 min at 4°C, and the supernatant was collected. Retinal supernatant was added to the ATP assay mix (catalog No. FLAAM, Sigma-Aldrich), diluted 1:625 with an ATP assay mix dilution buffer (catalog No. FLAAB, Sigma-Aldrich), and the luminescence signal generated by the oxidation of D-luciferin to oxyluciferin was immediately recorded with an Enspire Multimode Plate Reader. ATP values were calculated and expressed as nmol/mg protein.

Glutamate and glutamine concentration: Total glutamate and glutamine concentrations were measured using a commercial assay kit (Glutamine/Glutamate-Glo Assay, catalog No. J8022, Promega, Madison, WI). Each retina was placed in homogenization buffer comprised of 50 mM Tris (pH 7.5) buffer and 0.6N HCl inactivation solution II. The samples were then homogenized, and 600 mM Tris solution (pH 8.5) was added. The samples were then incubated with or without glutaminase for 40 min, after which glutamate detection reaction mixture (comprised of 50 µl of the Ultra-Glo™ rLuciferase solution, 0.25 µl of reductase, 0.25 µL of reductase substrate, 1 µl of glutamate dehydrogenase, and 1 µl of NAD per reaction) was added and incubated in dark conditions at room temperature for 60 min. Luminescence generated by the reduction of pro-luciferin to luciferin after NADH generation was recorded with an Enspire Multimode Plate Reader, and concentration values were normalized against protein concentration as measured by the Pierce 660-nm Protein Assay (Catalog no. 22,660/22662, Thermo Scientific, Waltham, MA). The differences in total glutamate concentration after glutaminase addition (glutamate + glutamine) and glutamate concentration without glutaminase addition (glutamate) were calculated to obtain the glutamine concentration. Concentrations were measured in triplicate and expressed as µmol/mg protein.

Silver-intensified immunogold labeling and quantification: Silver-intensified immunogold labeling was performed as previously described [7,25-29]. In brief, after fixation and resin embedding, eyecups were sectioned at 500 nm using a Leica Ultracut UCT ultramicrotome (Lecia Microsystems, Wetzlar, Germany). The sections were labeled with rabbit polyclonal anti-glutamate (1:500; ab9440, Abcam, Cambridge, UK), rabbit polyclonal anti-glutamine (1:500; ab9445, Abcam), rabbit polyclonal anti-GABA (1:100; ab9446, Abcam), and rabbit polyclonal anti-glycine (1:25; ab9442–500, Abcam). The secondary antibody used was a 1.4-nm Nanogold conjugated, IgG, goat anti-rabbit secondary antibody (1:100, No. 2003, GαR-gold, Nanoprobes, Yaphank, NY). The slides were then placed in a silver intensification solution in accordance with the method used by Moremans et al. [30] (60% distilled water, 0.02 M citrate buffer, 0.15% silver nitrate, and 0.03 M hydroquinone), in which silver ions are deposited onto the nanogold particle, causing samples with positive labeling to become visibly gray. Single WT and KO retinal sections were collected and treated with the same labeling solutions to ensure minimal difference in processing.

Silver-intensified immunogold labeling was visualized using a Leica DMR upright bright-field microscope (Leica Microsystems) with a Lecia DFC495 camera (Leica Microsystems) attachment. Images were captured at 300 dpi using the Leica Application Suite (LAS) software (version 4.8, Leica Microsystems) under a ×40 magnification oil immersion objective lens. The images were captured in grayscale using a digital camera attachment with a fixed exposure time of 65.8 ms and a gain of 5.4. At least six images from the central retina were taken for each label, age, and genotype.

Amino acid distributions were quantified using the ImageJ software (Version 1.50i; National Institute of Health, Bethesda, MD), as previously described [28]. In brief, the histogram tool was used to measure the average pixel intensity (ranging from 0 [black] to 255 [white]) of a fixed, 97-pixel circular area of interest. Regions of interest were captured from across the whole width of a layer, and the intracellular areas were recorded close to the middle of the somata to

reduce any preference toward greater or lesser staining. Pixel intensity was normalized against background labeling in each section, and the values were plotted as a ratio of KO/WT. Ten to 30 samples of average pixel intensity were obtained from the GC layer, MC endfeet (MCef), inner plexiform layer (IPL), amacrine cells (AC), MC bodies (MC), BP cells, outer plexiform layer (OPL), outer nuclear layer (ONL), photoreceptor inner segments (IS), and photoreceptor outer segments (OS).

Darker staining corresponds to higher levels of immunoreactivity, while lighter staining indicates lower levels of reactivity, allowing for quantitative analysis of changes in the neurochemical profiles. Differences in pixel intensity were presented as the fold-change in pixel intensity in the KO retinas relative to the WT retinas (whereby a result of 1.0 represents a 100% increase in labeling intensity in the KO retinas compared with the WT retinas [31], while a result of 0.0 represents equal labeling intensity in KO retinas compared with WT retinas), assuming that the pixel values from the WT retinas were a direct measure of amino acid concentrations in the retina [26].

Statistical analyses: For biochemical assays, each value represents the mean value normalized to the retinal protein concentration and is presented as mean ± standard error of the mean (SEM). For immunogold labeling, each value represents the mean difference in immunoreactivity relative to the control condition and is presented as the ratio of change ± SEM. Statistical comparison was performed using one-way (silver-intensified immunogold labeling) or two-way (biochemical assays) analysis of variance (ANOVA). Either the post hoc Dunnett's multiple comparison test or Tukey's multiple comparisons test for biochemical assays was used to compare each data point with the control data points for immunogold labeling. All statistical analysis was performed using GraphPad Software (Boston, MA), and a p value < 0.05 was considered statistically significant. Major increments of statistical significance are displayed as *$p < 0.05$, **$p < 0.01$, ***$p < 0.001$, or ****$p < 0.0001$.

RESULTS

Loss of xCT does not affect LDH activity or ATP concentration: The alterations in glutamate release in the xCT KO mice may have an impact on both the pre- and post-synaptic metabolisms due to the varied uses of glutamate in metabolic pathways. To test this, energy metabolism was assessed at the LDH activity level, as this is a key glycolytic enzyme whose activity helps in maintaining the high energy demand of the retina. LDH activity and ATP concentration were not significantly different between the WT and xCT KO retinas at 6 weeks, 3 months, 6 months, 9 months, and 12 months of age.

Figure 1A shows no significant differences in LDH activity according to age (WT: 6 weeks vs 3 months, $p = 0.0005$; 6 months, $p = 0.4742$; 9 months, $p > 0.9999$; and 12 months, $p > 0.9999$; KO: 6 weeks vs 3 months, $p < 0.0001$; 6 months, $p = 0.0034$; 9 months, $p = 0.8007$; and 12 months, $p = 0.6906$) or between the WT and xCT KO retinas for each age group (6 weeks, $p = 0.9715$; 3 months, $p > 0.9999$; 6 months, $p = 0.9968$; 9 months, $p = 0.1963$; and 12 months, $p > 0.9999$). These results suggest that the LDH activity was unaffected by the loss of xCT function.

As glutamate can enter the TCA cycle when there is energy demand, we investigated whether the total ATP production changed in the absence of a functional xCT transporter. Figure 1B shows no significant differences in ATP concentration between the WT and xCT KO retinas according to age (WT: 6 weeks vs 3 months, $p > 0.9999$; 6 months, $p = 0.8398$; 9 months, $p > 0.9999$; and 12 months, $p = 0.4948$; KO: 6 weeks vs 3 months, $p > 0.9999$; 6 months, $p = 0.9986$; 9 months, $p = 0.9985$; and 12 months, $p = 0.9166$) or between genotypes for each age group (6 weeks, $p > 0.9999$; 3 months, $p > 0.9999$; 6 months, $p = 0.9879$; 9 months, $p > 0.9999$; and 12 months, $p = 0.9932$). While there appeared to be higher ATP concentrations in the 6- and 12-month xCT KO retinas than in the WT retinas, the difference was not significant. Taken together, the loss of xCT function in the xCT KO retinas did not induce any significant alterations to the retinal glycolytic metabolism and aerobic glycolysis.

Loss of xCT does not alter the glutamate and glutamine concentrations in the whole retina: If xCT is involved in glutamate export from the photoreceptor, then loss of xCT function might lead to changes in the neurochemical balance of glutamate and glutamine, which are linked to the glutamate-glutamine cycle [7]. To test this, we measured glutamate and glutamine concentrations in WT and xCT KO retinas at 6 weeks, 3 months, 6 months, 9 months, and 12 months of age.

Figure 2A shows no significant differences in glutamate concentration for the WT and xCT KO retinas according to age (WT: 6 weeks vs 3 months, $p = 0.9744$; 6 months, $p = 0.5355$; 9 months, $p > 0.9999$; and 12 months, $p > 0.9999$; KO: 6 weeks vs 3 months, $p > 0.9999$; 6 months, $p = 0.9045$; 9 months, $p = 0.9642$; and 12 months, $p = 0.9995$) or between the genotypes for each age group (6 weeks, $p > 0.9999$; 3 months, $p = 0.9456$; 6 months, $p > 0.9999$; 9 months, $p = 0.9941$; 12 months, $p = 0.9973$).

Figure 2B shows no significant differences in glutamine concentration in the WT and xCT KO retinas according to

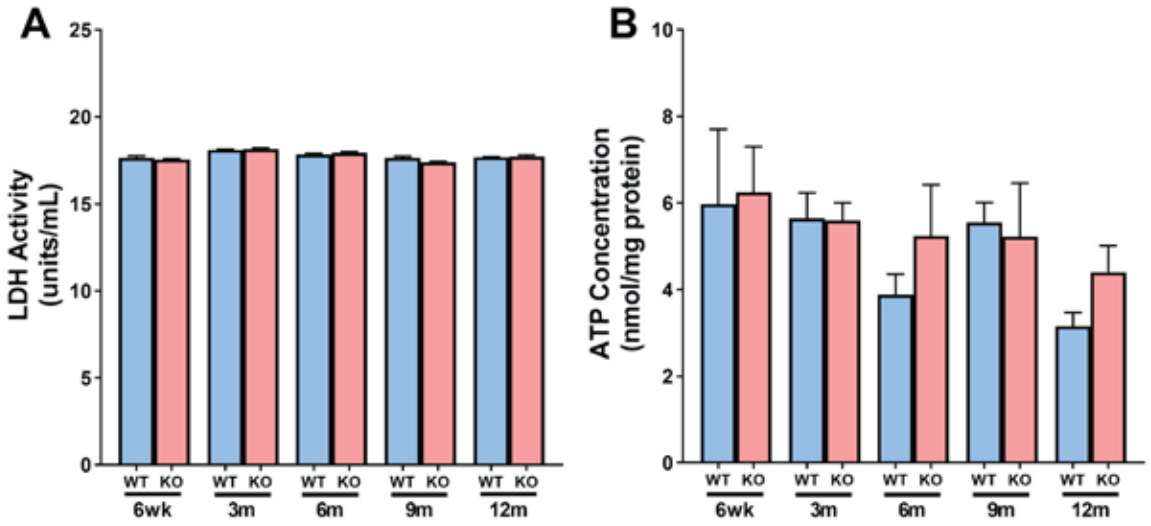

Figure 1. LDH activity and ATP concentrations in the retina. WT and xCT KO retinal homogenates were collected and measured for LDH activity (A) or ATP concentrations (B) in 6-week, 3-month, 6-month, 9-month, and 12-month-old WT (blue) and xCT KO (red) mice. Values represent mean ± SEM (n = 6).

age (WT: 6 weeks vs 3 months, p = 0.9984; 6 months, p = 0.2077; 9 months, p > 0.9999; 12 months, p > 0.9999; KO: 6 weeks vs 3 months, p > 0.7629; 6 months, p = 0.9145; 9 months, p > 0.9999; and 12 months, p = 0.8314) or between the genotypes for each age group (6 weeks, p = 0.8156; 3 months, p = 0.9961; 6 months, p > 0.9999; 9 months, p = 0.6594; and 12 months, p > 0.9999).

Compared with the glutamate concentrations, the glutamine concentrations were lower in the whole retina (approximately twofold less), which reflects that only the retinal MCs can synthesize glutamine and that glutamine is rapidly metabolized back into glutamate [32]. Nevertheless, loss of xCT function appeared not to induce any significant

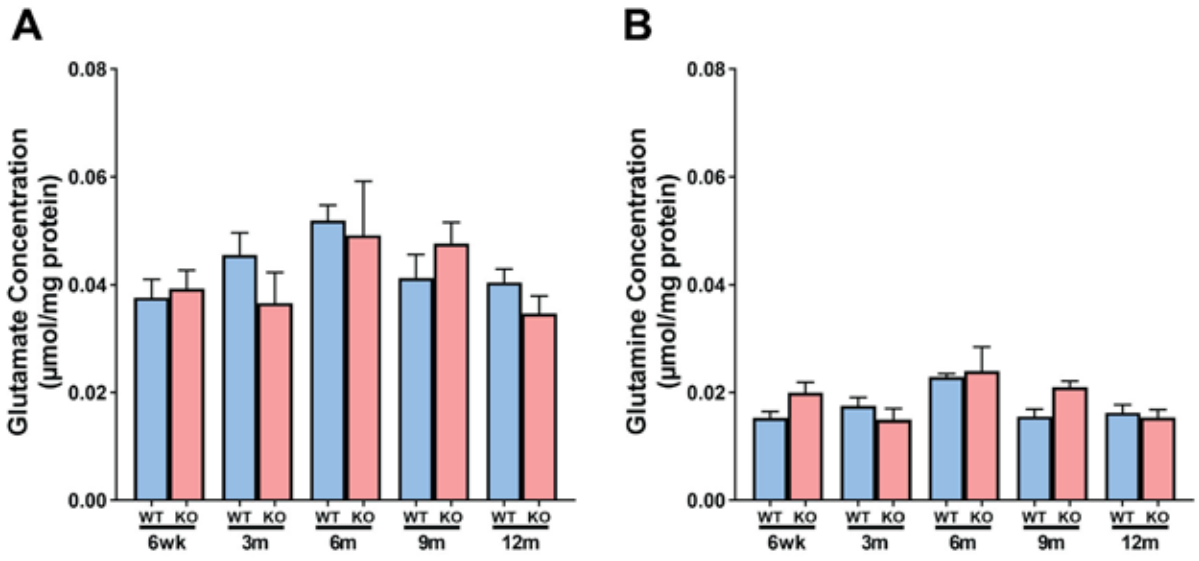

Figure 2. Glutamate and glutamine concentrations in the retina. WT and xCT KO retinal homogenates were collected, and total concentrations of glutamate or glutamine (glutamate + glutamine) were measured using a luminescence assay. (A) Total retinal glutamate concentrations in 6-week, 3-month, 6-month, 9-month, and 12-month-old WT (blue) and xCT KO (red) mice. (B) Total retinal glutamine concentrations for 6-week, 3-month, 6-month, 9-month, and 12-month-old WT (blue) and xCT KO (red) mice. Values represent mean ± SEM (n = 6).

alterations to the overall glutamate and glutamine concentrations in the whole retina.

Loss of xCT alters glutamate and glutamine levels in specific cell types of the retina: While no changes in glutamate and glutamine concentrations were found in whole retinas, the specific localization of xCT in the OPL of the retina [20] suggests that rather than affecting the whole retina, changes may be restricted to specific cell types in the outer retina such as the photoreceptors. To investigate this, post-embedding silver-intensified immunocytochemistry [26,33] was used to map and quantify glutamate and other glutamate-related amino acids such as glutamine, GABA, and glycine to the level of individual retinal cells in 6-week and 9-month-old WT and xCT KO retinas. The 9-month age group was selected because at this age, the xCT KO mice demonstrated signs of accelerated aging in the retina, likely due to photoreceptor oxidative damage [21].

Glutamate levels increase in the photoreceptors: To determine if the loss of the glutamate export function of xCT significantly affected the cellular glutamate distribution, the retinas were labeled with an anti-glutamate antibody. Figure 3A shows that the 6-week-old WT retinas exhibited glutamate immunoreactivity in nearly all retinal neurons, with particularly high reactivity in the photoreceptors, BP cells, and GCs that form the primary retinal signal transmission pathway, and lower levels of glutamate immunoreactivity in horizontal and ACs. MC bodies (dark arrows) show almost no immunoreactivity for glutamate owing to their ability to rapidly convert glutamate into glutamine in normal retina. Figure 3C shows that in the 6-week xCT KO retina, lighter staining was observed in the BP cells and GCs relative to the WT retina, indicating lower glutamate levels in the cells involved in the signaling pathway downstream of the photoreceptors. The outer and inner photoreceptor segments, and the outer nuclear and outer plexiform layers show darker staining in the xCT KO retinas than in the WT retinas, indicating accumulation of glutamate in areas upstream of the photoreceptor synapses at the OPL. Figure 3E shows the quantitative analysis of the glutamate labeling of the xCT KO retinas compared with the WT retinas, indicating that the xCT KO retinas had a significant increase in glutamate immunoreactivity in the OPL (100% ± 15%; p = 0.0157), ONL (38% ± 9%; p = 0.0052), and photoreceptor inner segment (132% ± 11%; p = 0.0105) compared with the WT retinas. This suggests that loss of xCT results in glutamate accumulation within the photoreceptor cell, particularly in the inner segments where the mitochondria are located, and potentially toward the presynaptic bouton. No changes in glutamate immunoreactivity were observed in the BP cells or GCs.

Analysis of glutamate labeling in the 9-month WT and xCT KO retinas also revealed differences in glutamate immunoreactivity, most notably in the OPL (Figure 3B,D). The quantitative analysis result (Figure 3F) confirmed a significant increase in glutamate labeling in the OPL (95% ± 27%, p = 0.0240) of the xCT KO retinas relative to the WT retinas. However, unlike the 6-week xCT KO retinas, the 9-month xCT KO retinas showed no increase in glutamate immunoreactivity in the ONL and inner segments. While it appeared that glutamate labeling was reduced in the xCT KO retinas compared with the WT in these layers, the difference was not statistically significant.

Glutamine levels decrease in MCs: As glutamine availability is dependent mainly on the glutamate uptake by MCs at the synaptic cleft and conversion of glutamate to glutamine, the glutamine distribution in the WT and xCT KO retinas was next investigated. The glutamine labeling in the 6-week WT retinas was most intense in the MC bodies and GCs (Figure 4A), consistent with previous reports [7,27]. Comparison between the 6-week WT and xCT KO retinas (Figure 4A, C) suggests a decrease in glutamine immunoreactivity in the MC bodies and an increase in glutamine immunoreactivity in the inner and outer photoreceptor segments. However, quantitative analysis revealed that the decrease in glutamine immunoreactivity in the MC bodies was the only significant difference (−53% ± 18%, p = 0.0101) between the xCT KO and WT retinas (Figure 4E).

Quantitative analysis of glutamine labeling in the 9-month retinas revealed a significant decrease in glutamine immunoreactivity in the MC bodies in the xCT KO retinas relative to the WT retinas (−43% ± 19%, p = 0.0144; Figure 4F). While glutamine immunoreactivity appeared to be increased in the ACs and MC endfeet in the xCT KO retinas compared with the WT retinas (Figure 4B,D), quantitative analysis confirmed that this was not statistically significant (Figure 4F).

GABA levels are unchanged by the loss of xCT function: As GABA is a known product of glutamate derived from glutamate decarboxylase and forms a branch of the glutamate-glutamine cycle [34,35], GABA distribution in the WT and xCT KO retinas was next investigated. The GABA labeling in the 6-week (Figure 5A) and 9-month (Figure 5B) WT retinas indicates a high degree of GABA immunoreactivity in the ACs, inner plexiform layer, and GCs, similar to published findings [7]. Comparison between the 6-week WT and xCT KO retinas (Figure 5A,C) and 9-month WT and xCT KO retinas (Figure 5B,D) showed increased GABA immunoreactivity in the inner plexiform layer and ACs in the xCT KO retinas relative to the WT retinas for both age groups.

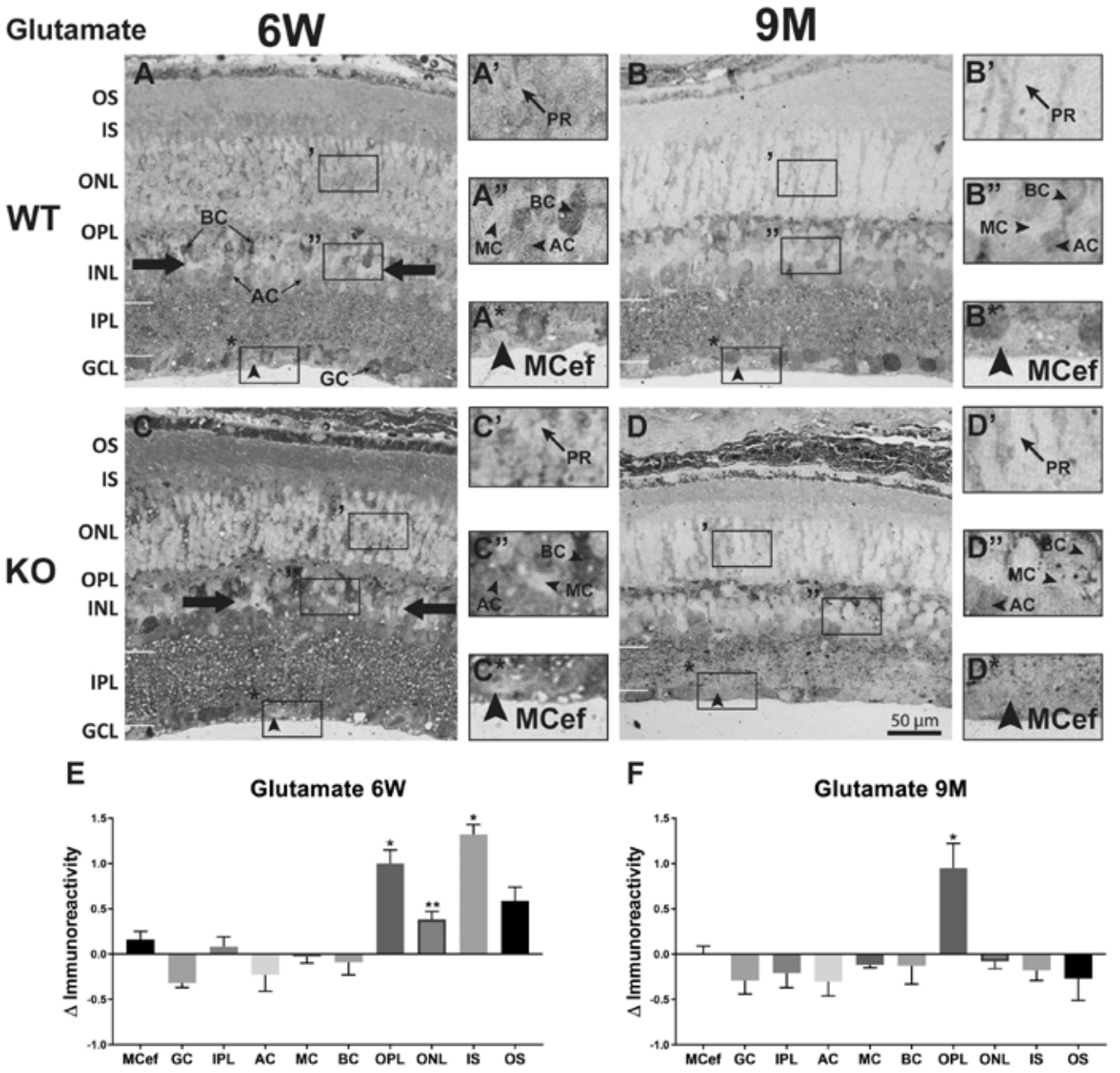

Figure 3. Silver-intensified immunogold staining for glutamate in 6-week and 9-month-old WT and xCT KO retinas. (A–D) Representative images of glutamate immunoreactivity in the 6-week WT (A) and xCT KO (C) retinas, and 9-month WT (B) and xCT KO (D) retinas. The dark arrows in (A) and (C) indicate Müller cells; the thinner arrows in (A) are examples of BP cells (BC), amacrine cells (AC), and ganglion cells (GC); and the individual arrowheads indicate the location of the Müller cell endfeet. Scale bar = 50 µm. Insets show magnified views of the outer nuclear layer (A'-D'), inner nuclear layer (A″–D″), and ganglion cell layer (A*–D*). The cell types identified in these views include the photoreceptor cell bodies (PR), BC, Müller cell bodies (MC), AC, and the Müller cell endfeet (MCef). (E and F) Quantitative analysis of glutamate in each retinal layer expressed as the percentage change in amino acid immunoreactivity of the 6-week xCT KO (C) or 9-month xCT KO (D) retinas in comparison with the age-matched WT retinas, whereby a change of 1 represents a 100% change in labeling intensity. OS=photoreceptor outer segments; IS=photoreceptor inner segments; ONL=outer nuclear layer; OPL=outer plexiform layer; INL=inner nuclear layer; IPL=inner plexiform layer; GCL=ganglion cell layer. n = 6 retinas. *p < 0.05, **p < 0.01.

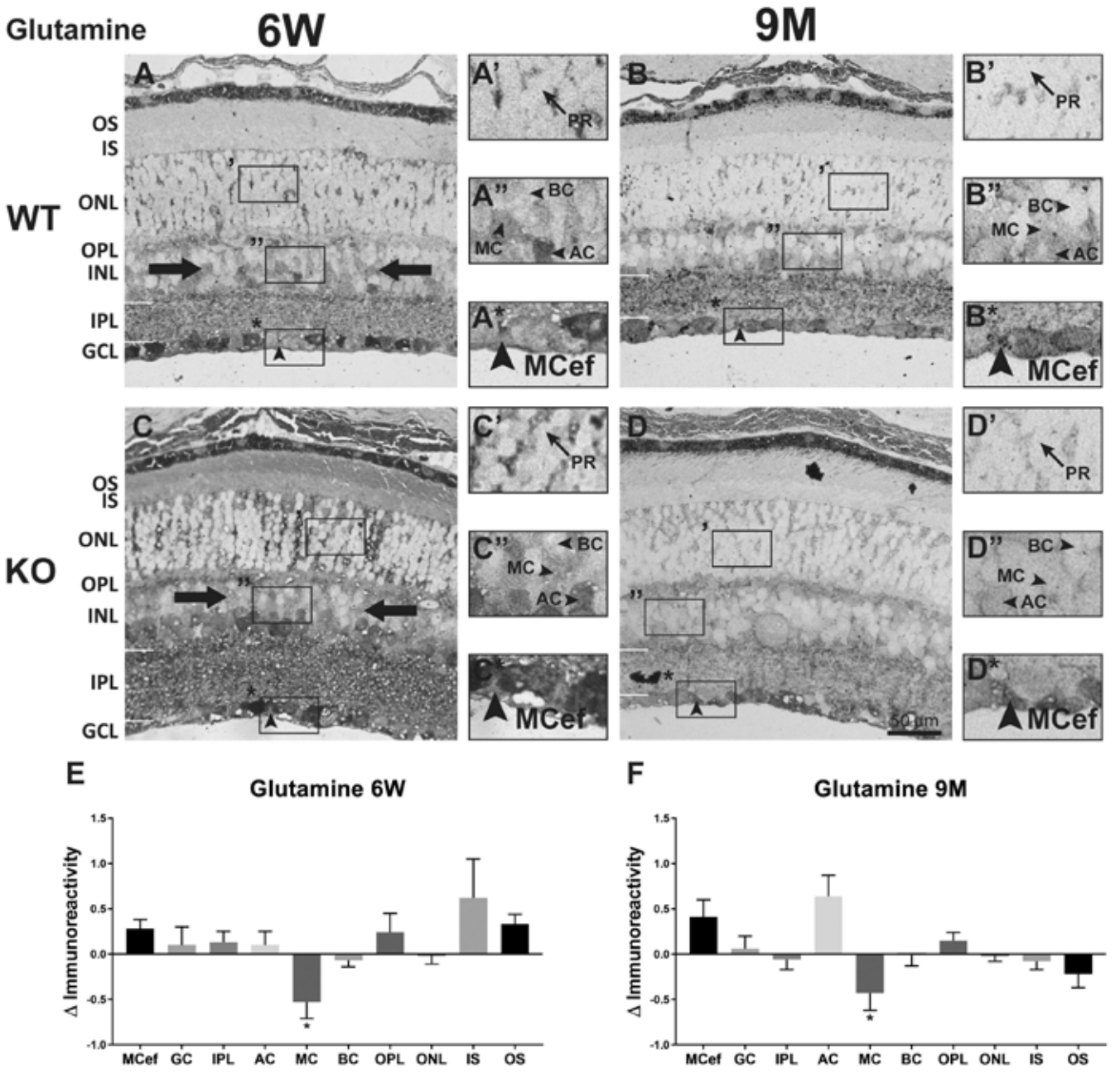

Figure 4. Silver-intensified immunogold staining for glutamine in 6-week and 9-month-old WT and xCT KO retinas. (A–D) Representative images of glutamine immunoreactivity in the 6-week WT (A) and xCT KO (C) retinas, and 9-month WT (B) and xCT KO (D) retinas. The dark arrows in (A) and (C) indicate Müller cells, and the individual arrowheads indicate the location of the Müller cell endfeet. Scale bar = 50 µm. Insets show magnified views of the outer nuclear layer (A′–D′), inner nuclear layer (A″–D″), and GC layer (A*–D*). The cell types identified in these views include the photoreceptor cell bodies (PR), bipolar cells (BC), Müller cell bodies (MC), amacrine cells (AC), and the Müller cell endfeet (MCef). (E and F) Quantitative analysis result of glutamate in each retinal layer expressed as the percentage change in amino acid immunoreactivity for the 6-week xCT KO (C) or 9-month xCT KO (D) retinas in comparison with the age-matched WT retinas. n = 6 retinas. *p < 0.05.

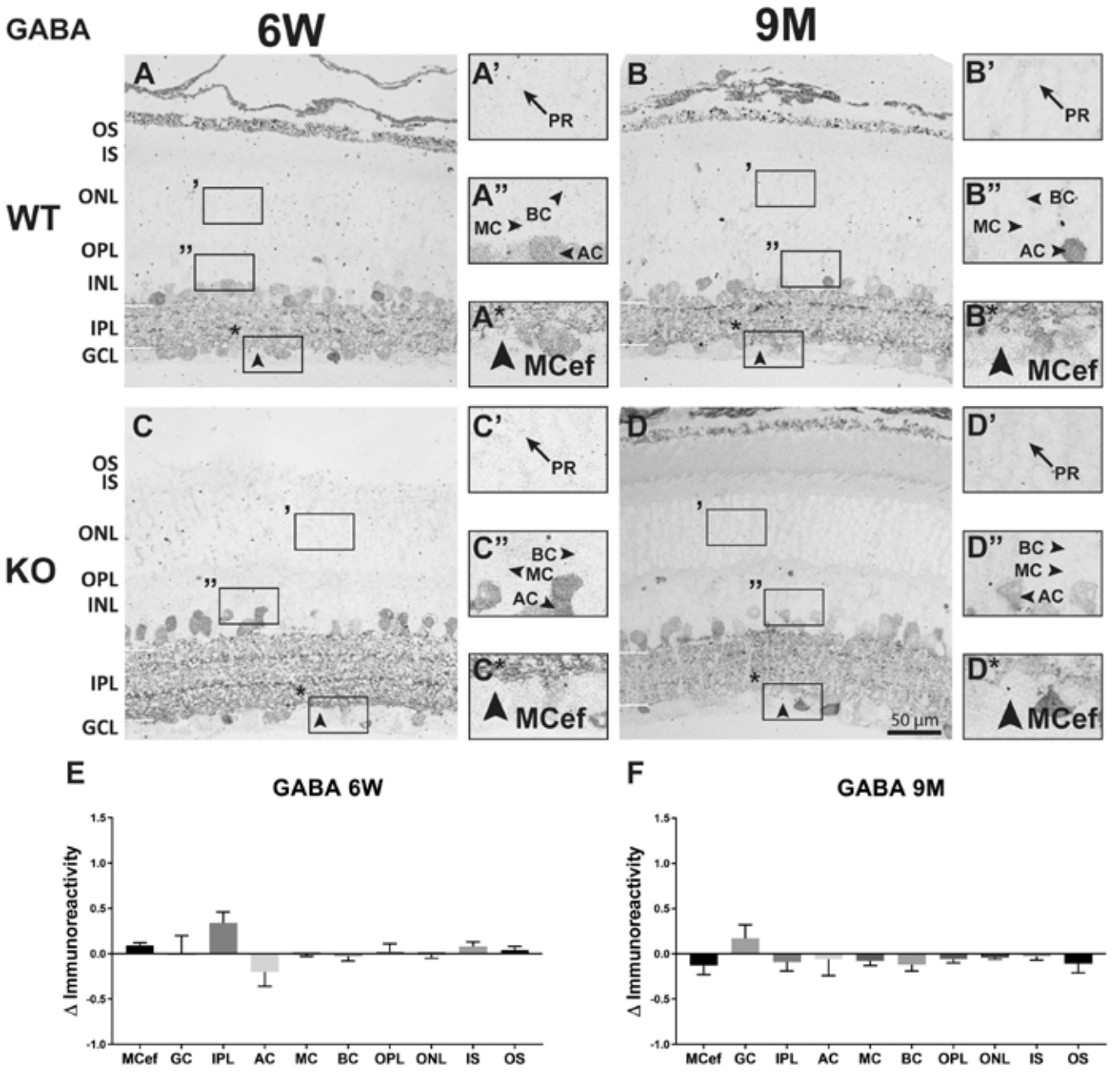

Figure 5. Silver-intensified immunogold staining for GABA in 6-week and 9-month-old WT and xCT KO retinas. (A–D) Representative images of GABA immunoreactivity in the 6-week WT (A) and xCT KO (C) retinas, and 9-month WT (B) and xCT KO (D) retinas. The individual arrowheads indicate the location of the MC endfeet. Scale bar = 50 µm. Insets show magnified views of the outer nuclear layer (A′–D′), inner nuclear layer (A″–D″), and ganglion cell layer (A*–D*). The cell types identified in these views include the photoreceptor cell bodies (PR), bipolar cells (BC), Müller cell bodies (MC), amacrine cells (AC), and the Müller cell endfeet (MCef). (E and F) Quantitative analysis result of glutamate in each retinal layer expressed as the percentage change in amino acid immunoreactivity for the 6-week xCT KO (C) or 9-month xCT KO (D) retinas in comparison with the age-matched WT retinas. n = 6 retinas.

However, quantitative analysis revealed no significant changes in GABA concentration between any of the retinal layers of the 6-week WT and xCT KO retinas (Figure 5E) or between the 9-month WT and xCT KO retinas (Figure 5F). These results indicate that the loss of xCT does not alter GABA concentrations in the retina.

Glycine levels are unchanged by the loss of xCT function: Glycine is an inhibitory neurotransmitter released from ACs that opposes glutamate excitatory action [36], particularly on downstream BP cells and GCs [37]. In addition, as it is known that in the brain, presynaptic glycine receptors can enhance glutamate release [38], glycine immunoreactivity in the WT and xCT KO retinas was investigated.

Glycine labeling in the 6-week (Figure 6A) and 9-month WT retinas (Figure 6B) indicated a high degree of glycine immunoreactivity in the ACs, similar to published findings [39]. Comparison of labeling patterns between the 6-week WT and xCT KO retinas suggested a decrease in glycine labeling in the ACs and inner plexiform layer in the xCT KO retinas (Figure 6A,C) and increased labeling in the OPL and inner and outer segments, whereas the opposite was observed in the 9-month retinas, with increased AC labeling and decreased labeling in the OPL and inner and outer segment in the xCT KO retinas compared with the WT retinas (Figure 6B–D). However, quantitative analysis revealed no significant differences in glycine labeling in any of the retinal layers between the WT and xCT KO retinas at 6 weeks (Figure 6E) or 9 months of age (Figure 6F). These results show that glycine concentrations were unaffected by the loss of xCT.

DISCUSSION

As xCT is involved in the export of glutamate, we hypothesized that a loss of xCT function would influence presynaptic metabolism of photoreceptors and postsynaptic levels of glutamate and derivated neurotransmitters. To test this, experiments were performed to determine if glycolysis was upregulated, as minor changes in TCA cycle demand can have an effect on LDH activity and ATP. The results of this study suggest that while loss of xCT function and abnormal glutamate release does not appear to affect the metabolic demand through connection with metabolic glutamate, this does impact the glutamate-glutamine cycle, as removal of xCT resulted in significant changes to the glutamate and glutamine distributions between the photoreceptor cells and the MCs. On the other hand, it appears unlikely that glutamate export by xCT plays a significant role in influencing downstream inhibitory cells such as GABAergic and glycinergic ACs, as no significant changes in either GABA or glycine labeling was detected between the WT and KO retinas for both age groups.

Metabolic role of xCT: Given that xCT exports glutamate and that the glutamate skeleton may be used in the TCA cycle via anaplerotic reactions in conditions of metabolic imbalance [40-42], it was expected that loss of xCT function would disrupt glutamate homeostasis and downregulate upward glycolytic pathways. However, no changes in the activity of LDH, the enzyme that converts lactate to pyruvate to maintain the high energy demand of the retina through glycolysis, or in ATP levels according age or between genotypes.

No significant differences in retinal LDH activity between WT and xCT KO mice were detected, which suggests that loss of xCT does not affect the lactate metabolism in mice up to 12 months of age. However, these mice may be more reliant on anaplerotic reactions that utilize substrates such as glutamate, aspartate, and valine to replenish TCA cycle intermediates without the need for pyruvate to maintain energy production [40]. Consistent with no significant changes in LDH activity reported in previous studies in normal mice at these ages [43], no significant changes in ATP levels were found with age or between the WT and xCT KO mice for any age group. ATP concentrations typically decline with age [44]; therefore, this may be revealed in older age groups than those included in this study.

LDH expression and activity decrease in an age-dependent manner in tissues such as the brain, heart, skeletal muscle, and liver [45]. However, no other studies have measured LDH activity in the retinas of aging mice. As the upper limit of the average life span of C57BL/6J mice is approximately 28–32 months [46,47], it may be that retinal LDH activity in older mice may be required to detect decreased LDH activity.

Both LDH activity and ATP concentrations were measured in whole retinal homogenates. Given that localized changes to glutamate and glutamine concentrations in specific cell types were detected, localized changes in LDH activity and ATP production in the photoreceptor cells cannot be ruled out. At this stage, however, no evidence shows that loss of xCT function directly impacts glycolytic metabolism.

Influence of xCT on neurochemical distributions: While no significant changes in overall glutamate and glutamine concentrations were found in the xCT KO retinas compared with the age-matched WT retinas, loss of xCT was associated with localized changes in glutamate and glutamine distribution. Initially, it was thought that removal of a glutamate export system would lead to a decrease in released glutamate. It was found that glutamate was increased in the photoreceptor

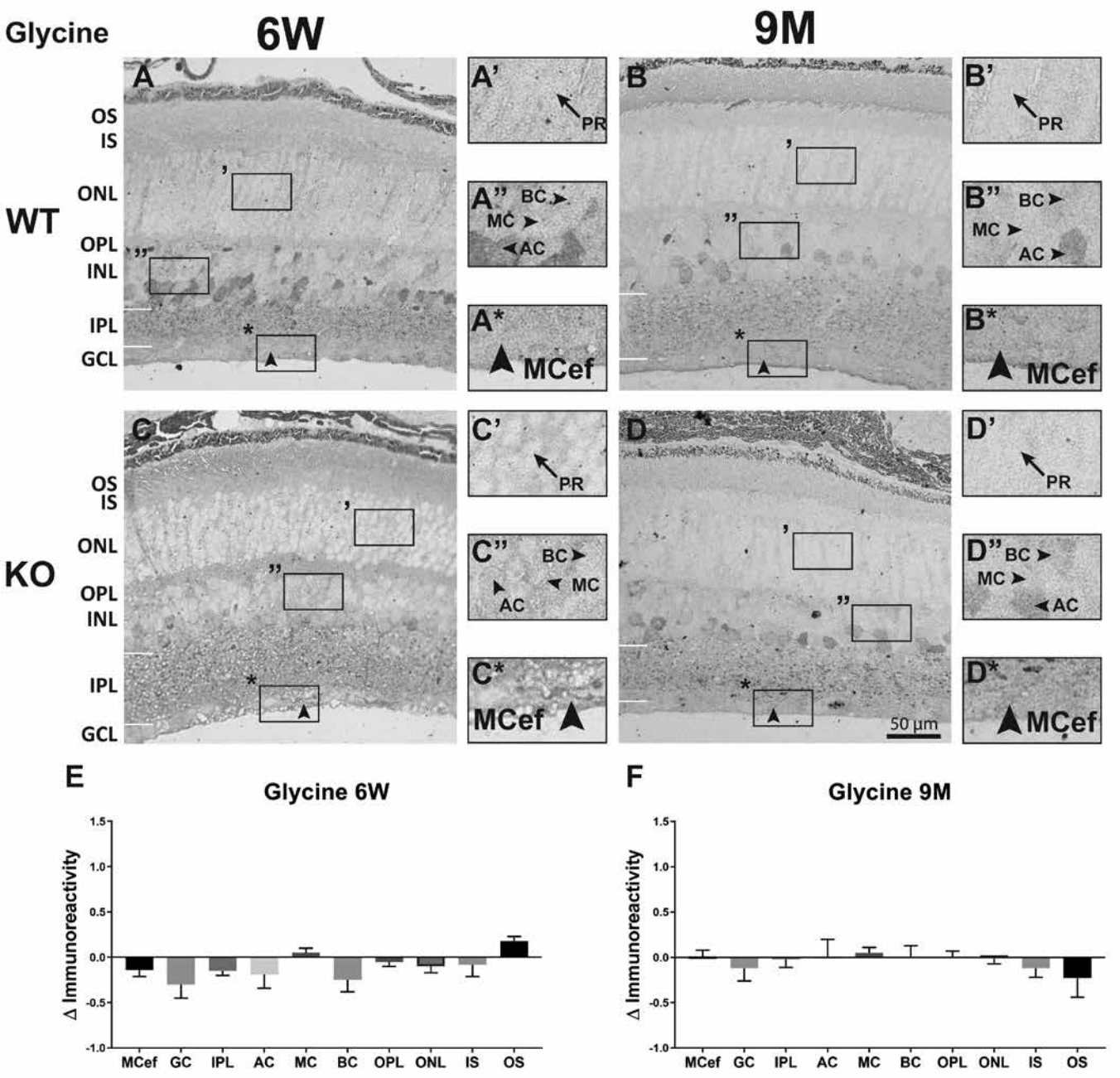

Figure 6. Silver-intensified immunogold labeling of glycine in 6-week and 9-month-old WT and xCT KO mice. (A–D) Representative images of glycine immunoreactivity in the 6-week WT (A) and xCT KO (C) retinas, and 9-month WT (B) and xCT KO (D) retinas. The individual arrowheads indicate the location of the Müller cell endfeet. Scale bar = 50 µm. Insets show magnified views of the outer nuclear layer (A′–D′), inner nuclear layer (A″–D″), and ganglion cell layer (A*–D*). The cell types identified in these views include the photoreceptor cell bodies (PR), bipolar cells (BC), Müller cell bodies (MC), amacrine cells (AC), and the Müller cell endfeet (MCef). (E and F) Quantitative analysis result of glutamate in each retinal layer expressed as the percentage change in amino acid immunoreactivity for the 6-week xCT KO (C) or 9-month xCT KO (D) retinas in comparison with the age-matched WT retinas. n = 6 retinas.

inner/outer segment, nuclear layer, and OPL, areas occupied by photoreceptors. However, the average mouse OPL thickness is approximately 19.22 ± 4.34 µm [48], and the optimal synaptic cleft separation distance is approximately 12–20 nm [49]. Therefore, it is likely that the immunogold light-based microscopy technique simply does not possess the resolution to accurately discriminate between glutamate labeling in the photoreceptor presynaptic ribbons; the horizontal, Müller, or BP cell postsynaptic boutons; or the outer plexiform synaptic cleft itself [50,51]. In nuclear layers, however, labeling was more definitive and demonstrated glutamate immunoreactivity to be specifically increased in the photoreceptor cell bodies of the ONL and the photoreceptor inner segments, indicating that the loss of the glutamate export function of xCT results in a significant accumulation of glutamate within the photoreceptor cell. Therefore, these findings demonstrate that xCT plays a major role in the export of glutamate into the outer plexiform layer, which contains the photoreceptor synapses, similar to some reports of xCT activity in the central nervous system [17-19].

In addition to the accumulation of glutamate in the photoreceptors, we also observed a depletion of glutamine in the MC bodies of the xCT KO retinas compared with the WT retinas. This is not a surprising finding given the connection between glutamine and glutamate through the glutamate-glutamine cycle [7], in which glutamate released from the photoreceptors is taken up by the MCs and rapidly converted into glutamine by the enzyme glutamine synthetase [10] before being exported into neurons. The MCs are the only cells that contain the glutamine synthetase enzyme and are therefore capable of converting glutamate to glutamine. In these cells, a significant decrease in glutamine immunoreactivity in the xCT KO retinas was observed at both 6 weeks and 9 months of age. A reduction in glutamine levels in the MCs implies that either these cells are receiving reduced glutamate supply leading to lower glutamine production or MCs increase their glutamine export into the extracellular space for photoreceptor reuptake [52]. As no significant changes in glutamine levels were found in the OPL of the xCT KO retinas, it is likely that MC glutamine production is reduced, which suggests that xCT is a significant exporter of glutamate from the photoreceptor cells.

Potential influence of xCT on non-glutamatergic neurotransmission: Previous studies have shown that glutamate exported from the photoreceptors via xCT may induce the closure or opening of cation channels in postsynaptic BP cells and induce BP cell hyperpolarization/depolarization in the same manner as traditional synaptic neurotransmission via vesicular release [20]. GABA can be transanimated to succinate for use in the TCA cycle [53,54] or converted to glutamate via anaplerotic reactions after TCA cycle NADH production [55]. Meanwhile, glycine is known to potentiate *N*-methyl-D-aspartate (NMDA) receptor-mediated current and is also a cotransmitter in excitatory NMDA synapses [56]. As BP cells can be activated by xCT-released glutamate and synapse with GABAergic and glycinergic ACs [37,57-59], xCT may indirectly regulate downstream GABAergic and glycinergic release [37]. However, loss of xCT function resulted in no significant differences in GABA or glycine immunoreactivity in the xCT KO retinas at 6 weeks or 9 months of age. The accumulation of glutamate in the photoreceptors of the xCT KO retina does not affect GABA production, consistent with the fact that despite being a related metabolite to glutamate, GABA is not produced in photoreceptors but only in ACs [37] in this species. While glutamate appears to be significantly released by xCT, its effect on the synapse may be too small to induce changes in the downstream GABAergic or glycinergic signaling pathways.

In summary, these findings provide evidence for the role of xCT as a significant exporter of glutamate in maintaining the glutamate-glutamine cycle between the photoreceptor cells and the MCs. While at the whole tissue level, glycolytic and energetic pathways appeared unaffected, it is likely that localized changes in energy metabolism occur in line with localized changes in glutamate and glutamine distributions. In our future work, we plan to investigate the role of xCT in its ability to uptake cyst(e)ine for the synthesis of glutathione and examine how this may impact antioxidant homeostasis in the retina. Moreover, as loss of xCT results in the accumulation of glutamate within the photoreceptor axon terminals and inner segments, which coincide with areas of high mitochondria content [60], it will be interesting to study the impact of this on mitochondrial function.

ACKNOWLEDGMENTS

The authors declare no conflicts of interest. This work was funded through grants supplied by the Auckland Medical Research Foundation 1115008, 1116006; The New Zealand Optometric Vision Research Foundation 3712086, The University of Auckland 3719594, 3708252, 3703162.

REFERENCES

1. Poitry-Yamate CL, Poitry S, Tsacopoulos M. Lactate released by Müller glial cells is metabolized by photoreceptors from mammalian retina. J Neurosci 1995; 15:5179-91. [PMID: 7623144].

2. Winkler BS, Arnold MJ, Brassell MA, Sliter DR. Glucose dependence of glycolysis, hexose monophosphate shunt

activity, energy status, and the polyol pathway in retinas isolated from normal (nondiabetic) rats. Invest Ophthalmol Vis Sci 1997; 38:62-71-[PMID: 9008631].

3. Johnson J, Fremeau RT Jr, Duncan JL, Rentería RC, Yang H, Hua Z, Liu X, LaVail MM, Edwards RH, Copenhagen DR. Vesicular glutamate transporter 1 is required for photoreceptor synaptic signaling but not for intrinsic visual functions. J Neurosci 2007; 27:7245-55. [PMID: 17611277].

4. Brandstätter JH, Koulen P, Wässle H. Diversity of glutamate receptors in the mammalian retina. Vision Res 1998; 38:1385-97. [PMID: 9667006].

5. Wong-Riley MT. Energy metabolism of the visual system. Eye Brain 2010; 2:99-116. [PMID: 23226947].

6. Tani H, Dulla Chris G, Farzampour Z, Taylor-Weiner A, Huguenard John R, Reimer Richard J. A Local Glutamate-Glutamine Cycle Sustains Synaptic Excitatory Transmitter Release. Neuron 2014; 81:888-900. [PMID: 24559677].

7. Kalloniatis M, Tomisich G. Amino acid neurochemistry of the vertebrate retina. Prog Retin Eye Res 1999; 18:811-66. [PMID: 10530752].

8. Norenberg MD, Martinez-Hernandez A. Fine structural localization of glutamine synthetase in astrocytes of rat brain. Brain Res 1979; 161:303-10. [PMID: 31966].

9. Pow DV, Robinson SR. Glutamate in some retinal neurons is derived solely from glia. Neuroscience 1994; 60:355-66. [PMID: 7915410].

10. Riepe RE, Norenburg MD. Müller cell localisation of glutamine synthetase in rat retina. Nature 1977; 268:654-5. [PMID: 19708].

11. Schousboe A, Scafidi S, Bak LK, Waagepetersen HS, McKenna MC. Glutamate metabolism in the brain focusing on astrocytes. Adv Neurobiol 2014; 11:13-30. [PMID: 25236722].

12. Starr MS. Evidence for the compartmentation of glutamate metabolism in isolated rat retina J Neurochem 1974; 23:337-44. [PMID: 4153731].

13. Bridges RJ, Lutgen V, Lobner D, Baker DA. Thinking outside the cleft to understand synaptic activity: contribution of the cystine-glutamate antiporter (System xc-) to normal and pathological glutamatergic signaling. Pharmacol Rev 2012; 64:780-802. [PMID: 22759795].

14. Bannai S, Takada A, Kasuga H, Tateishi N. Induction of cystine transport activity in isolated rat hepatocytes by sulfobromophthalein and other electrophilic agents. Hepatology 1986; 6:1361-8. [PMID: 3793012].

15. Warr O, Takahashi M, Attwell D. Modulation of extracellular glutamate concentration in rat brain slices by cystine-glutamate exchange. J Physiol 1999; 514:783-93. [PMID: 9882750].

16. Cavelier P, Attwell D. Tonic release of glutamate by a DIDS-sensitive mechanism in rat hippocampal slices. J Physiol 2005; 564:397-410. [PMID: 15695241].

17. Baker DA, Xi Z-X, Shen H, Swanson CJ, Kalivas PW. The Origin and Neuronal Function of In Vivo Nonsynaptic Glutamate. J Neurosci 2002; 22:9134-41. [PMID: 12388621].

18. De Bundel D, Schallier A, Loyens E, Fernando R, Miyashita H, Van Liefferinge J, Vermoesen K, Bannai S, Sato H, Michotte Y, Smolders I, Massie A. Loss of System xc− Does Not Induce Oxidative Stress But Decreases Extracellular Glutamate in Hippocampus and Influences Spatial Working Memory and Limbic Seizure Susceptibility. J Neurosci 2011; 31:5792-803. [PMID: 21490221].

19. Massie A, Schallier A, Kim SW, Fernando R, Kobayashi S, Beck H, De Bundel D, Vermoesen K, Bannai S, Smolders I, Conrad M, Plesnila N, Sato H, Michotte Y. Dopaminergic neurons of system x(c)$^{-}$-deficient mice are highly protected against 6-hydroxydopamine-induced toxicity. FASEB J 2011; 25:1359-69. [PMID: 21191088].

20. Hu RG, Lim JC, Donaldson PJ, Kalloniatis M. Characterization of the cystine/glutamate transporter in the outer plexiform layer of the vertebrate retina. Eur J Neurosci 2008; 28:1491-502. [PMID: 18973574].

21. Martis RM, Knight LJ, Acosta ML, Black J, Ng R, Ji LCL, Donaldson PJ, Lim JC-H. Early onset of age-related changes in the retina of cystine/glutamate antiporter knockout mice. Exp Eye Res 2023; 227:109364[PMID: 36586548].

22. Sato H, Shiiya A, Kimata M, Maebara K, Tamba M, Sakakura Y, Makino N, Sugiyama F, Yagami K-i, Moriguchi T, Takahashi S, Bannai S. Redox Imbalance in Cystine/Glutamate Transporter-deficient Mice. J Biol Chem 2005; 280:37423-9. [PMID: 16144837].

23. Martis RM, Donaldson PJ, Li B, Middleditch M, Kallingappa PK, Lim JC. Mapping of the cystine–glutamate exchanger in the mouse eye: a role for xCT in controlling extracellular redox balance. Histochem Cell Biol 2019; 152:293-310. [PMID: 31396687].

24. Mattapallil MJ, Wawrousek EF, Chan C-C, Zhao H, Roychoudhury J, Ferguson TA, Caspi RR. The Rd8 Mutation of the Crb1 Gene Is Present in Vendor Lines of C57BL/6N Mice and Embryonic Stem Cells, and Confounds Ocular Induced Mutant Phenotypes. Invest Ophthalmol Vis Sci 2012; 53:2921-7. [PMID: 22447858].

25. Kalloniatis M, Fletcher EL. Immunocytochemical localization of the amino acid neurotransmitters in the chicken retina. J Comp Neurol 1993; 336:174-93. [PMID: 7902364].

26. Marc RE, Liu WL, Kalloniatis M, Raiguel SF, van Haesendonck E. Patterns of glutamate immunoreactivity in the goldfish retina. J Neurosci 1990; 10:4006-34. [PMID: 1980136].

27. Kalloniatis M, Tomisich G, Marc RE. Neurochemical signatures revealed by glutamine labeling in the chicken retina. Vis Neurosci 1994; 11:793-804. [PMID: 7918229].

28. Shivashankar G, Lim JC, Acosta ML. Proinflammatory cytokines trigger biochemical and neurochemical changes in mouse retinal explants exposed to hyperglycemic conditions. Mol Vis 2020; 26:277-90. [PMID: 32300272].

29. Shivashankar G, Lim JC, Acosta ML. Glyceraldehyde-3-phosphate dehydrogenase and glutamine synthetase inhibition in the presence of pro-inflammatory cytokines contribute to the metabolic imbalance of diabetic retinopathy. Exp Eye Res 2021; 213:108845[PMID: 34800480].

30. Moeremans M, Daneels G, Van Dijck A, Langanger G, De Mey J. Sensitive visualization of antigen-antibody reactions in dot and blot immune overlay assays with immunogold and immunogold/silver staining. J Immunol Methods 1984; 74:353-60. [PMID: 6209340].

31. Acosta ML, Kalloniatis M. Short- and long-term enzymatic regulation secondary to metabolic insult in the rat retina. J Neurochem 2005; 92:1350-62. [PMID: 15748154].

32. Poitry S, Poitry-Yamate C, Ueberfeld J, MacLeish PR, Tsacopoulos M. Mechanisms of glutamate metabolic signaling in retinal glial (Müller) cells. J Neurosci 2000; 20:1809-21. [PMID: 10684882].

33. In't Veld PA. Immunogold-silver labeling in histology. Am J Anat 1989; 185:321-6. [PMID: 2476025].

34. Hertz L. The Glutamate-Glutamine (GABA) Cycle: Importance of Late Postnatal Development and Potential Reciprocal Interactions between Biosynthesis and Degradation. Front Endocrinol 2013; 4:59-[PMID: 23750153].

35. Hertz L, Peng L, Dienel GA. Energy Metabolism in Astrocytes: High Rate of Oxidative Metabolism and Spatiotemporal Dependence on Glycolysis/Glycogenolysis. J Cereb Blood Flow Metab 2007; 27:219-49. [PMID: 16835632].

36. Marc RE. The role of glycine in the mammalian retina. Prog Retin Res 1988; 8:67-107. .

37. Wu SM, Maple BR. Amino acid neurotransmitters in the retina: a functional overview. Vision Res 1998; 38:1371-84. [PMID: 9667005].

38. Kunz PA, Burette AC, Weinberg RJ, Philpot BD. Glycine receptors support excitatory neurotransmitter release in developing mouse visual cortex. J Physiol 2012; 590:5749-64. [PMID: 22988142].

39. Fletcher EL, Kalloniatis M. Neurochemical architecture of the normal and degenerating rat retina. 1996; 376(3):343–60.

40. Owen OE, Kalhan SC, Hanson RW. The key role of anaplerosis and cataplerosis for citric acid cycle function. J Biol Chem 2002; 277:30409-12. [PMID: 12087111].

41. McGivan JD, Chappell JB. On the metabolic function of glutamate dehydrogenase in rat liver. FEBS Lett 1975; 52:1-7. [PMID: 1123072].

42. Korla K, Mitra CK. Modelling the Krebs cycle and oxidative phosphorylation. J Biomol Struct Dyn 2014; 32:242-56. [PMID: 23528175].

43. Acosta ML, Fletcher EL, Azizoglu S, Foster LE, Farber DB, Kalloniatis M. Early markers of retinal degeneration in rd/rd mice. Mol Vis 2005; 11:717-28. [PMID: 16163270].

44. Gkotsi D, Begum R, Salt T, Lascaratos G, Hogg C, Chau K-Y, Schapira AHV, Jeffery G. Recharging mitochondrial batteries in old eyes. Near infra-red increases ATP. Exp Eye Res 2014; 122:50-3. [PMID: 24631333].

45. Singh S, Kanungo M. Alterations in lactate dehydrogenase of the brain, heart, skeletal muscle, and liver of rats of various ages. J Biol Chem 1968; 243:4526-9. [PMID: 4300867].

46. Graber TG, Kim J-H, Grange RW, McLoon LK, Thompson LV. C57BL/6 life span study: age-related declines in muscle power production and contractile velocity. Age (Dordr) 2015; 37:9773-[PMID: 25893911].

47. Kunstyr I, Leuenberger HG. Gerontological data of C57BL/6J mice. I. Sex differences in survival curves. J Gerontol 1975; 30:157-62. [PMID: 1123533].

48. Ferguson LR, Dominguez Ii JM, Balaiya S, Grover S, Chalam KV. Retinal Thickness Normative Data in Wild-Type Mice Using Customized Miniature SD-OCT. PLoS One 2013; 8:e67265[PMID: 23826252].

49. Savtchenko LP, Rusakov DA. The optimal height of the synaptic cleft. Proc Natl Acad Sci USA 2007; 104:1823-8. [PMID: 17261811].

50. Cajal SR. Dieoe Retina der Wirbeltiere. Wiesbaden1894.

51. Kolb H, Nelson R, Mariani A. Amacrine cells, bipolar cells and ganglion cells of the cat retina: A Golgi study. Vision Res 1981; 21:1081-114. [PMID: 7314489].

52. Umapathy NS, Li W, Mysona BA, Smith SB, Ganapathy V. Expression and Function of Glutamine Transporters SN1 (SNAT3) and SN2 (SNAT5) in Retinal Müller Cells. Invest Ophthalmol Vis Sci 2005; 46:3980-7. [PMID: 16249471].

53. Tunnicliff G. 4-Aminobutyrate Transaminase. In: Boulton AA, Baker GB, Yu PH, editors. Neurotransmitter Enzymes. Totowa, NJ: Humana Press; 1986. p. 389–420.

54. Baxter CF. The Nature of γ-Aminobutyric Acid. In: Lajtha A, editor. Metabolic Reactions in the Nervous System. Boston, MA: Springer US; 1970. p. 289–353.

55. Roon RJ, Even HL, Larimore F. Glutamate synthase: properties of the reduced nicotinamide adenine dinucleotide-dependent enzyme from Saccharomyces cerevisiae. J Bacteriol 1974; 118:89-95. [PMID: 4362465].

56. Nong Y, Huang Y-Q, Ju W, Kalia LV, Ahmadian G, Wang YT, Salter MW. Glycine binding primes NMDA receptor internalization. Nature 2003; 422:302-7. [PMID: 12646920].

57. Watt CB, Li H-B, Lam DM-K. The presence of three neuroactive peptides in putative glycinergic amacrine cells of an avian retina. Brain Res 1985; 348:187-91. [PMID: 2866019].

58. Vaney DI, Young HM. GABA-like immunoreactivity in cholinergic amacrine cells of the rabbit retina. Brain Res 1988; 438:369-73. [PMID: 3345446].

59. O'Malley DM, Sandell JH, Masland RH. Co-release of acetylcholine and GABA by the starburst amacrine cells. J Neurosci 1992; 12:1394-408. [PMID: 1556600].

60. Stone J, van Driel D, Valter K, Rees S, Provis J. The locations of mitochondria in mammalian photoreceptors: Relation to retinal vasculature. Brain Res 2008; 1189:58-69. [PMID: 18048005].